

Workflows for Ultra-High Resolution 3D Models of the Human Brain on Massively Parallel Supercomputers

Hartmut Mohlberg^{1(✉)}, Bastian Tweddell², Thomas Lippert²,
and Katrin Amunts^{1,3}

¹ Institute of Neuroscience and Medicine (INM-1),
Research Centre Juelich and JARA-Brain, 52428 Jülich, Germany
`{h.mohlberg,k.amunts}@fz-juelich.de`

² Juelich Supercomputing Centre (JSC), IAS, and JARA-HPC,
Research Centre Juelich, 52428 Jülich, Germany
`{b.tweddell,th.lippert}@fz-juelich.de`

³ C. and O. Vogt Institute of Brain Research,
Heinrich-Heine University, 40225 Düsseldorf, Germany
`k.amunts@uni-duesseldorf.de`

Abstract. Human brain atlases [1] are indispensable tools to achieve a better understanding of the multilevel organization of the brain through integrating and analyzing data from different brains, sources, and modalities while considering the functionally relevant topography of the brain [4]. The spatial resolution of most of these electronic atlases is in the range of millimeters, which does not allow the integration of the information at the level of cortical layers, columns, microcircuits or cells. Therefore, we introduced in 2013 the first BigBrain data set with a resolution of 20 μm isotropic. This data set allows to specify morphometric parameters of human brain organization, which serve as a “gold standard” for neuroimaging data obtained at a lower spatial resolution. It provides, in addition, an essential basis for realistic brain models concerning structural analysis and simulation [2]. For the generation of other, even higher-resolution data sets of the human brain, we developed an improved and more efficient data processing workflow employing high performance computing to 3D reconstruct histological data sets. To facilitate the analysis of intersubject variability on a microscopic level, the new processing framework was applied for reconstructing a second BigBrain data set with 7676 sections. Efficient data processing of a large amount of data sets with a complex nested reconstruction workflow using large number of compute nodes required optimized distributed processing workflows as well as parallel programming. A detailed documentation of the processing steps and the complex inter-dependencies of the data sets at each level of the multi-step reconstruction workflow was essential to enable transformations to images of the same histological sections obtained with even higher spatial resolution. We have addressed these challenges, and achieved efficient high throughput processing of thousands of images of histological sections in combination with sufficient flexibility, based on an effective, successive coarse-to-fine hierarchical processing.

Keywords: Ultra-high resolution brain models · BigBrain · Cytoarchitecture · Microstructure · High performance computing · Workflows · Human Brain Atlas

1 Introduction

The cerebral cortex of the human brain is a highly heterogeneous structure. It is segregated into cortical areas, which differ between each other in their cellular architecture, but also in their molecular composition, connectivity, function, and other aspects of brain organization [1]. By analyzing Nissl-stained histological sections with a light microscope, Korbinian Brodmann has observed at the beginning of the last century that every cortical area showed a characteristic cellular architecture (cytoarchitecture) specified by the spatial distribution of neurons, the presence of particular cell types, the clustering of cell bodies, and the formation of cortical layers (thickness, density, etc.), which run in parallel to the cortical surface [5]. Based on these differences Brodmann published a map with 43 cortical cytoarchitectonic areas in humans (Fig. 1a). He was convinced that each cortical area subserves a certain function, although this had not been demonstrated for the majority of brain areas in these days.

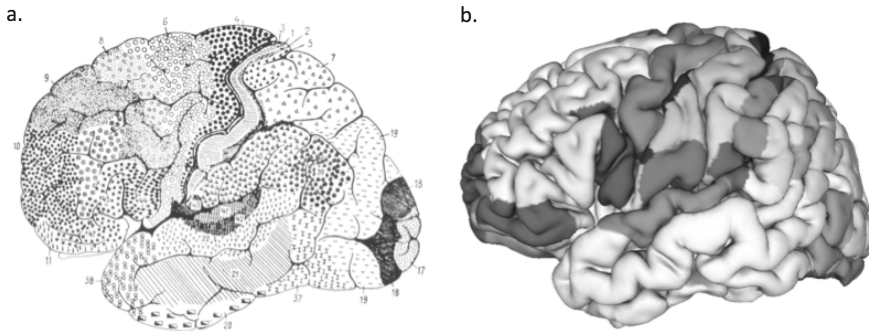


Fig. 1. (a) Brodmann's schematic map of the cerebral cortex of the human brain. Cortical areas are labeled with different patterns and numbers [5]. (b) Probabilistic JuBrain Atlas; areas are labeled by different gray values [17].

In contrast to the 2D map as drawn by Brodmann, the JuBrain atlas [17] represents a true 3D representation of cytoarchitectonic areas at a resolution of 1 mm isotropic, covers also areas buried in the depths of the sulci, and includes subcortical nuclei. In order to consider intersubject variability, each cytoarchitectonic area was mapped for 10 postmortem brains and has been 3D-reconstructed and normalized to the stereotaxic reference space of a single subject template provided by the Montreal Neurological Institute MNI [8]. As a result, probability maps could be calculated (e.g., [6]). The parcellation shown in Fig. 1b associates a label to that area, which had the highest probability at this particular

position in the atlas space (maximum probability map [7]). The combined analysis of modern in vivo neuroimaging studies and cytoarchitectonic probabilistic maps provides a deeper understanding of the role of cortical areas in complex brain functions including memory, language, abstraction, creativity, emotion and attention, and allows identifying networks of brain areas, which are involved in specific brain functions.

Such type of analyses of structure-functional relationships is constrained by the resolution of in vivo neuroimaging studies, which is in the millimeter range for the majorities of fMRI studies. This does not allow addressing the level of cortical layers, columns, and cells as structures relevant for brain activity and finally behavior. For this purpose, a resolution of $20\mu\text{m}$ and less is mandatory, which captures details of laminar and columnar organization. Going to even higher resolution, light microscopic images on a scale of $1\mu\text{m}$ allow detecting details of single cell morphology (for details see Fig. 2).

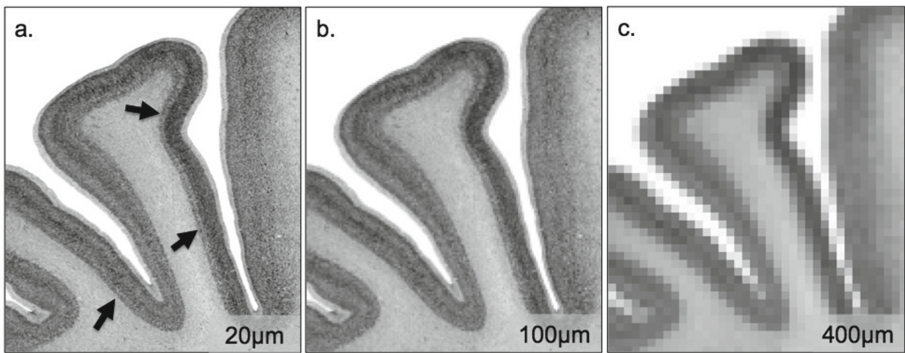


Fig. 2. Region of interest at various resolution levels. (a) A resolution of $20\mu\text{m}$ enables a reliable identification of cortical layers and their regional differences (marked by the arrows), columns and cells. This becomes increasingly more difficult at a resolution of $100\mu\text{m}$ (b) and is for most brain regions virtually impossible already at a resolution of $400\mu\text{m}$ (c). Note that even this resolution is still more than twice as high as those used in many fMRI studies.

In 2013 we have introduced the BigBrain data set [2] with a spatial resolution of $20\mu\text{m}$ isotropic. It is based on the 3D reconstruction of 7404 digitized histological sections, which were stained for cell bodies. This data set serves a new, microscopical reference space for neuroscience data and has become part of the HBP Human Brain Atlas [25]. In addition, it represents a basis for in-depths analyses of the cellular architecture. For example, the BigBrain data set has been used to extract parameters of brain organization such as cell densities, cortical thicknesses, the laminar pattern and cortical surface [14–16].

The generation of this BigBrain data set was extremely time-consuming and labor-intensive. Based on a 16-bit gray value coding, the total size of the original 7404 digitized histological sections with an in-plane resolution of $20\mu\text{m}$

was between 0.6 and 1 TiB. The processing workflow for the 3D reconstruction included several steps: the reconstruction of blockface images, the registration of MR images of the formalin fixed brain to blockface images (obtained during histological sectioning), linear and nonlinear 2D alignment of histological sections to corresponding sections of the aligned MR-images, volume-to-volume registration of MR-images to stacked histological sections, and section-to-section alignment of histological sections to each other or to MR images [2].

In addition, the workflow was considerably complicated by the fact that many images of the histological sections were not successively processed through each processing step, but processed differently, for example to correct for distortions and histological artifacts affecting the images in a different degree. Histological artifacts are inevitably accompanied by cutting large human brain sections, the mounting of sections on glass slides and staining. This becomes particularly relevant at very high spatial resolutions, where even smallest artifacts become visible. Up to 40 % of the images required (time consuming) manual repair. The removal of artifacts in subsets of images was done in an iterative manner, to improve consecutively the quality of the 3D reconstructed data set.

The complex dependencies of the various data sets demand an efficient data management and processing system. It should be capable to facilitate the processing of those subsets of images, where artifact correction has been carried out to avoid a repetitive processing of the whole series of histological sections. In addition, it is necessary to report carefully the corrections in order to provide a detailed documentation of the modifications applied to each image. This is a prerequisite for reproducibility, and a reliable interpretation of measurement results. Due to the large amount of data in combination with the complexity of the reconstruction workflow, the processing of the BigBrain data set requires advanced HPC technology for both data management and computing in order to speedup the image processing.

Here, we introduce an efficient HPC-adapted processing workflow to 3D-reconstruct histological data sets of the human brain with a high quality 20 μm resolution and with a scalability to be computed within a reasonable time frame. It includes a comprehensive documentation and provenance tracking of all processing steps as well as inter-dependencies of image and meta data at each level of the workflow. The new processing workflow was applied to 3D-reconstruct a new, second BigBrain data. The workflow has been developed on the multi-purpose HPC system JUROPA (Juelich Research on Petaflop Architectures) at the Juelich Supercomputing Centre (JSC). In 2015, it was necessary to migrate the complete workflow to JUROPA's successor JURECA (Juelich Research on Exascale Cluster Architectures).

2 Material and Overview of the Processing Workflow

A postmortem brain of a 30-year old male without any neurological or psychiatric diseases in clinical records was obtained through a body donor program in accordance to legal and ethical rules. It was fixed in 4 % buffered formalin

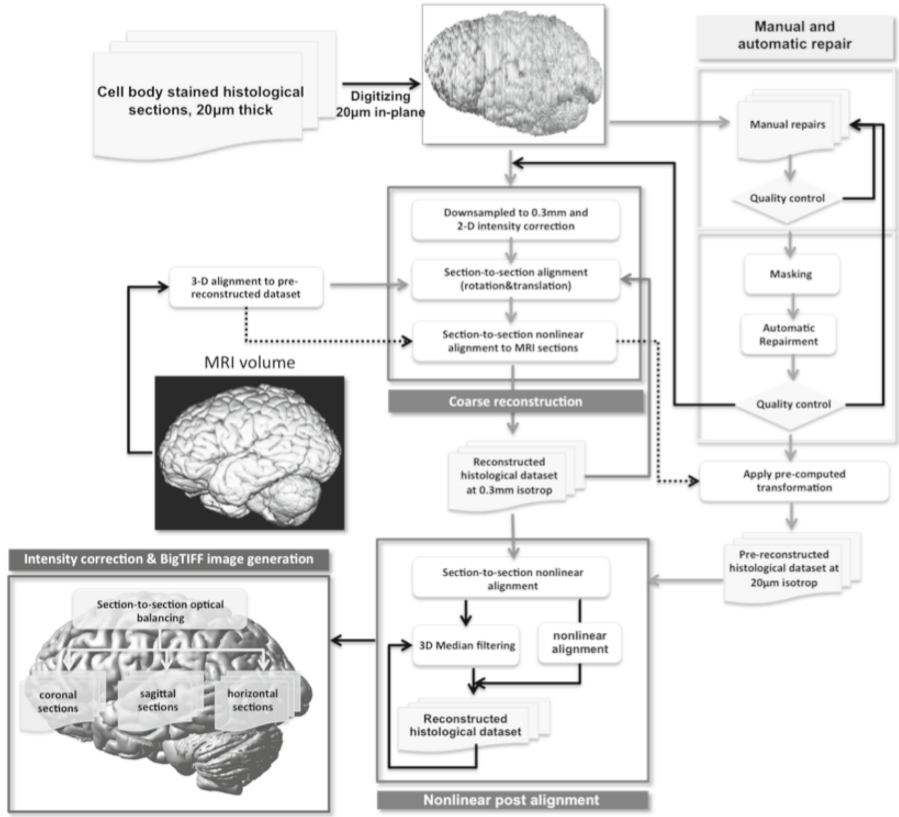


Fig. 3. HPC processing workflow for the 3D reconstruction of the second BigBrain data set. Gray colored boxes label different processing levels, which can be performed in parallel.

for several months. The fixed brain underwent MR-imaging with a resolution of $0.7 \times 0.7 \times 0.7$ mm. This MR data set served as an undistorted reference target for 3-dimensional reconstruction. The brain was embedded in paraffin, and serial coronal histological sections at $20 \mu\text{m}$ thickness were obtained with a large-scale microtome. 7676 sections were acquired, mounted, and stained for cell bodies. The stained sections were digitized using a flatbed scanner with a physical in-plane resolution of $10 \mu\text{m}$ and a dynamic range of 16 bits. All images were downsampled to $20 \times 20 \mu\text{m}$, framed to a uniform image size of 7000×6000 pixels and saved in png-format with lossless compression in order to generate an initial data set with isotropic resolution. All these steps were performed as described in our previous work [2]. In total, this raw data set occupied approximately 320 GiB of disk space.

To address the methodical data processing and managing challenges, we applied a simple, but efficient data provenance and tracking tool based on the

Open Provenance Model (OPM) [24] that provides a detailed and comprehensible documentation of all processing steps and data dependencies. The implementation permits a re-play of most of the processing scripts used for the first BigBrain data set. The tool does not require special prerequisites for the underlying hardware and software architecture and thus can be used both locally on a server as well as on a supercomputer. The processing steps include linear and nonlinear 2-dimensional alignments of histological sections to corresponding sections of the aligned MR images, volume-to-volume registration of MR images to stacked histological sections, section-to-section alignment of histological sections to each other or to MR images (Fig. 3). In contrast to our previous work, the new version specifies four interdependent processing levels executed in parallel. Sequentially executed processing steps are combined with those executed in parallel.

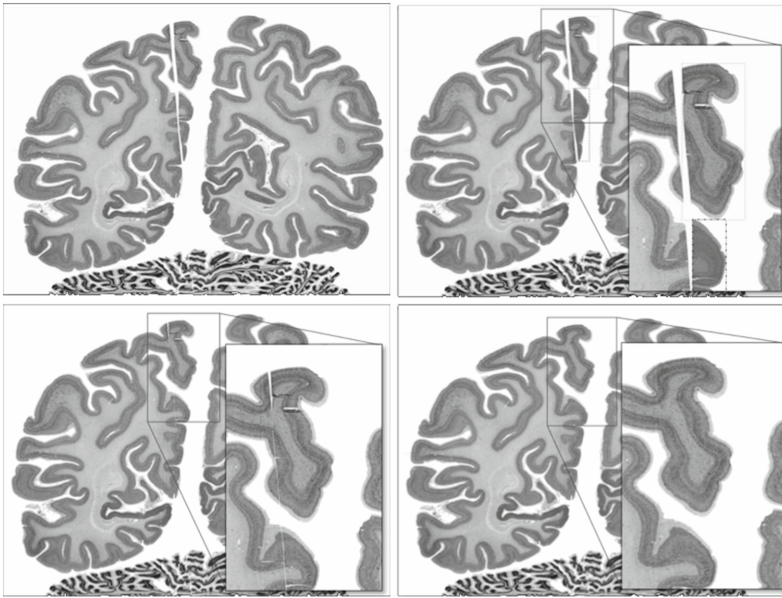


Fig. 4. Manual and automatic repair of displaced tissue pieces. Clockwise from top-left: Original section at $20\mu\text{m}$ resolution, manual labeled misaligned/damaged ROIs, manual corrected ROIs, and automatically corrected ROIs using neighboring sections [11]. All processing steps were automatically documented and stored in an xml-file. This file can later be applied to the same images, e.g., those scanned with higher spatial resolution.

Processing level (i): Manual and automatic repair. Images of histological sections differ in the presence of artifacts and the severity of the artifacts. They include e.g., rips, tears, staining artifacts, folds, missing and displaced pieces, with different size and constitution. Fully automatic methods often fail in removing such artifacts. Thus, time and labor intensive manual repair steps

are required. A trained expert can process approximately 20 to 30 sections per day. This manual repair is followed by an automatic artifact correction [11]. We have developed a new easy-to-use and effective tool, which also documents all steps (for some examples see Fig. 4).

Processing level (ii): Coarse reconstruction. A successive coarse-to-fine hierarchical framework was implemented for an efficient data processing and 3D-reconstruction, substantially accelerating the sequential data processing as used for the first BigBrain. A first coarse pre-reconstitution at a low in-plane resolution of 0.3 mm isotropic was computed, where the major part of the artifacts was negligible. Initially, every 15th section (section-to-section distance = 0.3 mm) was used, taking advantage of the postmortem MRI as an undistorted spatial reference [10]. The MRI was co-registered to this reconstructed histological data set and sampled up to the original number of sections using a B-spline imaging filter [13]. All down-sampled histological images were co-registered, section-by-section, to the coronal sections of the up-sampled co MR-volume using linear and non-linear registration tools [10]. Subsequently, the computed transformations were sampled up and applied to the original or to the repaired histological sections at a resolution of 20 μm . The second processing level was initially in parallel to the first level, but was re-executed, when new repaired sections were available. For example, the spatial resolution and the quality of the 3D-reconstruction were successively improved through newly incorporated repaired and corrected histological sections. In order to support this coarse-to-fine hierarchical processing, we employed a data flow management system, which provides an automatic monitoring of the processing steps and accounts for the complex dependencies of the data sets. In case of a modification of a certain number of input data sets only the modified images were re-computed, while non-modified data sets were not processed again.

Processing level (iii): Nonlinear post alignment. We computed at a (so far maximum) resolution of 40 μm a section-to-section nonlinear alignment. This step required up to 8 h of computation time per image, and was the computationally most expensive part. In order to improve the quality of the 3D-reconstruction, we computed for every image i the nonlinear alignment to the median image of its $i \pm 3$ neighbors thus reducing minor local misalignments.

Processing level (iv): Intensity corrections and BigTIFF image generation. Finally, a further section-to-section optical imbalance correction was computed. A 3D-volume file (320 GiB) was created. In addition, two virtual section planes in horizontal and sagittal directions were generated respectively. They were saved as tiled BigTIFF images on the global GPFS file system at the Jülich Supercomputing Centre which has a dedicated 1-Gbit/s-Ethernet connection to our local web server.

Quality control throughout the whole workflow is mandatory to guarantee high accuracy of the 3D-reconstruction. Artifacts are immediately visible in the two virtual section planes at high spatial resolution (i.e., horizontal and sagittal planes). They appear, for example, as distortions of the laminar pattern of the

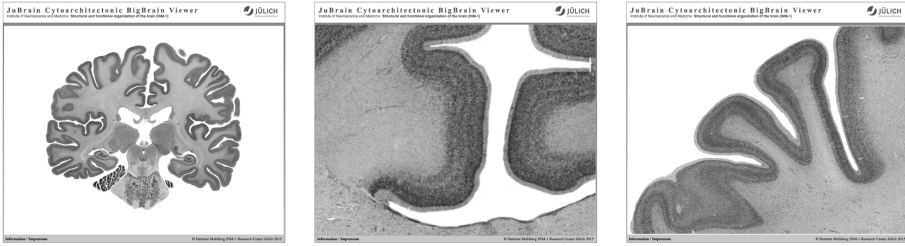


Fig. 5. Web-based online inspection of a processed histological section at different resolutions used for quality control.

cerebral cortex, or as distortions of the brain surface. Therefore, a web based visualization tool using the HTML5 standard was developed that is capable to visualize and explore even ultra-large tiled 2D data sets saved in the BigTIFF file format (see Fig. 5).

3 Computational Methods and Algorithms

In order to provide an automated workflow and data management system that efficiently utilizes advanced supercomputing infrastructures the provenance tracking systems documents every processing step automatically by creating a document file in xml data format. This document file contains detailed information about the compute node, the operating system, the time of creation, the software tools (name, revision, names of external library files, etc.), the processing parameters, and the input and output files (name, time, md5 checksum, etc.). Internally the workflow is implemented as a couple of Perl scripts, which call the executables that are written in C++. This was achieved by replacing the internal system command from Perl with a new, adapted system call command. By specifying program name, input options, name and type (regular or temporary file) of each input and output filename(s), the document file was automatically created for each output file and stored in its directory.

Data provenance and data management platforms become more important to facilitate a reproducible and effective neuroscience research [9]. The UNICORE (Uniform Interface to Computing Resources) grid middle ware offers a ready-to-run grid system that enables distributed computing on HPC and makes data resources available in a secure and user-friendly way in intranets and the internet [3]. However, like most of the platforms, it is not straightforward to integrate an already existing workflow package and to track all the processing steps carried out within the script. In order to meet the complexity of the present workflow and to re-use external workflow packages, we have developed a new in-house system. We used Python [18] powered by mpi4py [19] and graph-tool [20] for the programming of the processing workflows. In order to update a previously created data file, starting from the requested output file in a first run, a data dependency graph was created by backtracking and analyzing the created

log files of all input files. Only those images that had to be re-processed with respect to the modified input data (check based on existence, time creation and md5 checksum) were transmitted to the allocated compute nodes in a second run. The large number of processing steps and the interdependence of a large number of files resulted in a data dependency graph containing approximately 260,000 nodes. To reduce the complexity, we computed for each execution level a data dependency graph independently and connected the individual graphs afterwards.

The processing pipeline used to 3D reconstruct the first BigBrain data set was based on the prominent MINC tool kit, a comprehensive collection of individual programs for medical image processing and analysis [23]. Most of the included programs are very selective; in order to realize a more complex computation, often, multiple calls of a couple of different programs are required, which leads to a comparatively high I/O. In order to minimize I/O operations, successive computing algorithms and highly specialized C++ programs were developed, which are based on the Insight Segmentation and Registration Toolkit (ITK) [21] and an internal image processing library. A B-spline transformation model was used in combination with a Limited memory Broyden-Fletcher-Goldfarb-Shannon (L-BFGS-B) optimizer and a L2 metric [12] for the section-to-section alignment. The parameter space of the B-spline transformation was composed of the set of all the deformations associated with the nodes of the grid. Thus, a wide variety of deformations is considered, requiring a rather large amount of computation time. Specialized programs, parallelized with MPI-2, were developed since the ITK library does not support distributed processing by MPI-2 and cannot be used for very memory intensive programs. These programs allowed processing the complete BigBrain data volume with 320 GiB, which is a prerequisite to generate virtual sectioning planes. To save and read 3D data sets from storage, we used the HDF5 library that provides optimized parallel I/O based on the MPI-2 library [22]. To provide a fast data visualization, final output images were stored in BigTIFF format that supports a tiled data organization facilitating a rapid access to single tiles.

4 HPC Computations on JUROPA and JURECA

All development and computations were done at the Jülich Supercomputing Centre on the HPC-system JUROPA and then migrated to its successor JURECA. JUROPA had 3288 compute nodes each with 2 Intel Xeon X5570 (Nehalem-EP) 2.93 GHz quad-core processors and 24 GiB of main memory. Approximately 22 GiB of memory per node were available for applications. In total, this led to a complete system of 26,304 cores, 79 TiB main memory, a peak performance of 308 Teraflops and a Linpack performance of 274.8 Teraflops. The batch system for managing jobs was Moab with the underlying resource manager TORQUE. The JURECA system, where so far 15 % of the computations have been carried out, has 1872 compute nodes each with 2 Intel Xeon E5-2680 v3 (Haswell) 2.5 GHz 12-core processors and 128 GiB of main memory. In total, this led to a

complete system of 45,216 cores, 271 TiB main memory and a peak performance of 1.8 Petaflops. In contrast to JUROPA, the new system uses a Slurm batch system with Parastation resource management.

Python powered by mpi4py was used to implement the workflows, which scaled up well to the (so far) maximum allocation of 512 cores. Going from the bottom level to the highest stage of execution level that has already been reached for each execution level of the workflow, we executed a cold run, where no output files were generated. By analyzing previously created document files, the total number of images that had to be re-computed with respect to modified input data was determined. The required computation time was estimated using the documented execution time of the previous run. If no logging information was available, for example for the first run, the execution time was estimated based on past experience. Relative to the number of required computing cores and execution time, an appropriately adapted batch job was generated and sent to the batch system in a second run.

Each processing step was logged, including manual interventions. By analyzing data dependencies, only those images that had to be re-computed with respect to the modified original data were transmitted to the allocated compute nodes. The section-to-section, linear and nonlinear elastic alignment of all histological sections was hereby the most computational intensive part. For each section, the applied ITK registrations programs were called multiple times at different scale-levels with different parameter sets. In the more interactive, semi-automatic part of the removal of artifacts, only a limited number of sections (20) were processed at the same time whereas in the overall part all sections (7676) were affected. For most of our processing steps, each affected image was automatically transmitted by our data flow management system to a single core.

Table 1. Overview of the computation and processing time (including time spent for the manual repairs) for the individual processing levels presented in Fig. 3.

	Computation time	Processing time
Manual and automatic repair	20 %	85 %
Coarse reconstruction	5 %	1 %
Nonlinear post alignment	65 %	12 %
Intensity correction & BigTIFF image generation	10 %	2 %
In total	200,000 core-h	2.5 years

The maximum resolution for the nonlinear alignment, which was limited by the available amount of memory per core, was achieved on JUROPA at an in-plane resolution of 40 μm . In this case, the maximum amount of memory per core was about 2.1 GiB and was determined by the size of the input image, its internal data representation (which is unsigned integer), the number of internal scale levels (6 at maximum), the number and data representation of meta

images (e.g. mask images), and the size and data type (which is double) of the nonlinear deformation vector field. Consuming about 200,000 core hours in 2.5 years (see Table 1) about 580,000 data files requiring 3.5 TiB of disk space have been computed while the original version of the first BigBrain required more than 2,000,000 core-h and 5 years of processing. Full spatial resolution of $20\mu\text{m}$ will be achieved at JURECA where the work is continued.

5 Results

The second BigBrain has been 3D-reconstructed (Fig. 6). The quality of the reconstruction is high, as verified in the two virtual sectioning planes below. Minor structural imbalances are primarily due to the computation of the section-to-section alignment at a reduced resolution of $40\mu\text{m}$. They are currently corrected by re-computing the alignments at full resolution on JURECA.

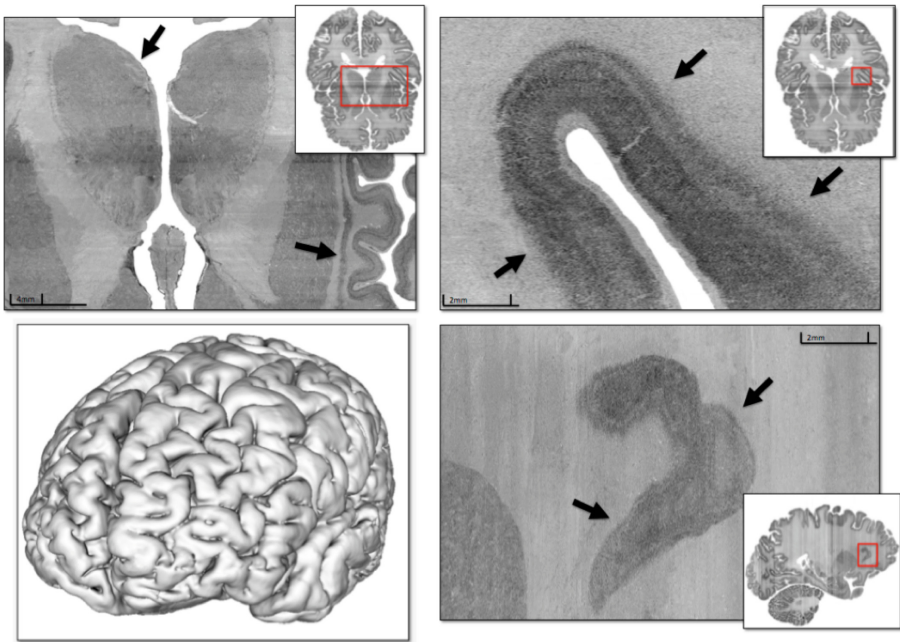


Fig. 6. Images of virtual section planes of the second BigBrain data. Note the smooth borders of the cerebral cortex and subcortical nuclei (arrow heads) in the virtual planes (horizontal upper row, sagittal lower right) as an indicator of the high quality of the 3D-reconstruction. The quality of the images is comparable to the results of the first BigBrain data set presented in 2013, but required much less computing time.

6 Conclusions

BigBrain data with microscopical resolutions are tools, that can be used by the neuroscience community for different purposes. They allow to generate morphometric parameters of brain organization, in form of an atlas, or can provide information for processing of in vivo data sets in order to constrain simulation. To facilitate the generation of such data sets, we have introduced a novel workflow for the 3D-reconstruction of serial histological sections using massively parallel supercomputers, thereby relying on our experience in generating the first BigBrain data set [2]. An efficient data processing performance is guaranteed by the data flow management system implemented that provides a detailed automatic documentation of the processing steps and the complex dependencies of the data sets at each level of the reconstruction workflow. In addition, this framework provides a necessary methodical prerequisite for future BigBrain data sets with even higher resolution. Such data sets pose significant challenges with respect to data handling, analysis, and storage capacities, i.e., Big Data Analytics. For example, images of whole brain histological sections scanned with 1 μm in-plane resolution and 16-bit gray value would result in an image size of up to $120,000 \times 100,000$ pixels and 18 GiB per image for the BigTIFF data format. Thus, the total raw data set of a single brain will require about 180 TiB of storage space. The storage space of a human brain data set at 1 μm isotropic will require several PiB. The workflow presented here opens new perspectives for analyzing human brain organization at the microscopical level.

Acknowledgments. The authors thank Claude Lepage and Alan C. Evans from the Montreal Neurological Institute, Montreal, Canada, for developing and providing the HPC workflow for the 3-D reconstruction of the first BigBrain, which served as a basis for the recent workflow and for many fruitful and inspiring discussions. We thank Ana Oros-Peusquens and Nadim J. Shah for their contribution in MR-imaging. Funding was provided for this study by the European Union Seventh Framework Programme (FP7/2007-2013) under grant agreement no. 604102 (Human Brain Project), and the Portfolio Theme Supercomputing and Modeling for the Human Brain of the German Helmholtz Association.

References

1. Zilles, K., Amunts, K.: Centenary of Brodmann’s map - conception and fate. *Nat. Rev. Neurosci.* **11**(2), 139–145 (2010)
2. Amunts, K., Lepage, C., Borgeat, L., Mohlberg, H., Dickscheid, T., Rousseau, M., Bludau, S., Bazin, P., Lewis, L., Oros-Peusquens, A., Shah, N., Lippert, T., Zilles, K., Evans, A.C.: BigBrain: an ultrahigh-resolution 3D human brain model. *Science* **340**, 1472–1475 (2013)
3. Amunts, K., Bücker, O., Axer, M.: Towards a multiscale, high-resolution model of the human brain. In: Grandinetti, L., Lippert, T., Petkov, N. (eds.) *Brain-Comp 2013. LNCS*, vol. 8603, pp. 3–14. Springer, Heidelberg (2014). doi:[10.1007/978-3-319-12084-3_1](https://doi.org/10.1007/978-3-319-12084-3_1)

4. Amunts, K., Hawrylycz, M., Van Essen, D., Van Horn, J.D., Harel, N., Poline, J.B., De Martino, F., Bjaalie, J.G., Dehaene-Lambertz, G., Dehaene, S., Valdes-Sosa, P., Thirion, B., Zilles, K., Hill, S.L., Abrams, M.B., Tass, P.A., Vanduffel, W., Evans, A.C., Eickhoff, S.B.: Interoperable atlases of the human brain. *Neuroimage* **99**, 525–532 (2014)
5. Brodmann, K.: Vergleichende Lokalisationslehre der Großhirnrinde in ihren Prinzipien dargestellt auf Grund des Zellbaues. Barth, Leipzig (1909)
6. Amunts, K., Malikovic, A., Mohlberg, H., Schormann, T., Zilles, K.: Brodmanns area 17 and 18 brought into stereotaxic space where and how variable? *Neuroimage* **11**(1), 66–84 (2000)
7. Eickhoff, S., Stephan, K.E., Mohlberg, H., Grefkes, C., Fink, G.R., Amunts, K., Zilles, K.: A new SPM toolbox for combining probabilistic cytoarchitectonic maps and functional imaging data. *Neuroimage* **25**(4), 1325–1335 (2005)
8. Evans, A.C., Janke, A.L., Collins, D.L., Baillet, S.: Brain templates and atlases. *Neuroimage* **62**(2), 911–922 (2012)
9. Delescluse, M., Franconville, R., Joucla, S., Lieurya, T., Pouzat, C.: Making neurophysiological data analysis reproducible. Why and how? *J. Physiol. Paris* **106**, 159–170 (2011)
10. Hömke, L.: A multigrid method for anisotropic PDEs in elastic image registration. *Numer. Linear Algebra Appl.* **13**, 215–229 (2006)
11. Lepage, C., Mohlberg, H., Pietrzyk, U., Amunts, K., Zilles, K., Evans, A.C.: Automatic repair of acquisition defects in reconstruction of histology slices of the human brain. In: 16th Annual Meeting of the Organization for Human Brain Mapping (OHBM), Barcelona, 06. - 10.06.2010: available on CD-ROM (2010)
12. Zhu, C., Byrd, R.H., Nocedal, L.: L-BFGS-B: Algorithm 778: L-BFGS-B, FORTRAN routines for large scale bound constrained optimization. *ACM Trans. Math. Softw.* **23**(4), 550–560 (1997)
13. Thévenaz, P., Blu, T., Unser, M.: Interpolation revisited. *IEEE Trans. Med. Imaging* **19**(7), 739–758 (2000)
14. Lewis, L., Lepage, C., Fournier, M., Zilles, K., Amunts, K., Evans, A.C.: BigBrain: Initial tissue classification and surface extraction. In: 20th Annual Meeting of the Organization for Human Brain Mapping (OHBM), Hamburg (2014)
15. Liu, S., Azevedo, C., Pelletier, D.: The use of BigBrain in MS: An ultrahigh-resolution 3D template for grey matter MRI segmentation. *Neurology* **82**(10), 6.135 (2014)
16. Wagstyl, K., Lepage, C., Zilles, K., Amunts, K., Fletcher, P., Evans, A.: BigBrain: Automated analysis of laminar structure in the cerebral cortex. In: 22nd Annual Meeting of the Organization for Human Brain Mapping (OHBM), Geneva (2016)
17. JuBrain Cytoviewer: <https://www.jubrain.fz-juelich.de/apps/cytoviewer/cytoviewer-main.php>
18. Python Software Foundation: Python Language Reference, Version 2.7. <http://www.python.org>
19. MPI for Python. <http://pypi.python.org/pypi/mpi4py>
20. Graph-tool: Efficient network analysis with Python. <http://www.graph-tool.org>
21. Insight Segmentation and Registration Toolkit (ITK). <http://www.itk.org>
22. The HDF Group: Hierarchical data format (HDF), Version 5. <http://www.hdfgroup.org/HDF5>
23. Minc Tool Kit. <http://www.bic.mni.mcgill.ca/ServicesSoftware/MINC>
24. The Open Provenance Model (OPM). <http://www.openprovenance.org>
25. The Human Brain Project (HBP). <https://www.humanbrainproject.eu>

Brain-Inspired Computing

Second International Workshop, BrainComp 2015,
Cetraro, Italy, July 6-10, 2015, Revised Selected Papers
Amunts, K.; Grandinetti, L.; Lippert, Th.; Petkov, N.
(Eds.)

2016, X, 195 p. 47 illus., Softcover

ISBN: 978-3-319-50861-0